Control Parameter Design for Hypersonic Vehicle via Improved Comprehensive Learning Pigeon-Inspired Optimization

Hongcheng Xiang and Yimin Deng(✉)

School of Automation Science and Electrical Engineering, Beihang University, Beijing 100083, China

ymdeng@buaa.edu.com

Abstract. In this paper, an Active Disturbance Rejection Control (ADRC) system is proposed to address the complex disturbance during the flight of Hypersonic Vehicle (HV). To deal with difficulties in the manual control parameter design task, an Improved Comprehensive Learning Pigeon-Inspired Optimization (ICLPIO) algorithm is utilized by converting the parameter design problem to an optimization problem. The comprehensive learning strategy and the selective learning mechanism are introduced to improve the convergence rate and exploration performance in the parameters tuning for ADRC system of HV. To verify the advantages of the ICLPIO algorithm, the particle swarm optimization (PSO), the basic PIO, and the genetic algorithm (GA) are applied in the simulations as control groups. The results show that the presented method is superior to other optimization methods.

Keywords: Active Disturbance Rejection Control (ADRC) · Hypersonic Vehicle (HV) · Pigeon-Inspired Optimization (PIO) · Comprehensive learning strategy

1 Introduction

The Hypersonic Vehicle (HV) has certain values in both military and civilian aspects due to its high speed [1]. Different from traditional aircrafts, more disturbance factors should be considered for HV, including serious nonlinear characteristic, the strong time variability brought about large airspace flight and hypersonic flow, and uncertainty caused by variable parameters and random interference [2]. As a key technology, the design of control system has a direct impact on flight performance of a HV system.

The Active Disturbance Rejection Control (ADRC) is a nonlinear control method, which has been explored and used to design fault tolerance controllers in many practical applications [3]. For aircraft attitude control, an adaptive ADRC system for small unmanned aerial vehicle (UAV) system processed excellent stability, rapidity, and accuracy [4]. For aircraft trajectory tracking control, an ADRC system was applied in the power parafoil aerial vehicle system and achieved required precision and disturbance-rejection capacity of instruction tracking [5]. In addition to aircraft control, applications

L. Yan et al. (Eds.): ICGNC 2022, LNEE 845, pp. 4020–4028, 2023.
https://doi.org/10.1007/978-981-19-6613-2_392

of ADRC in other system show competitive performance. With a new observer structure, an improved ADRC was used for a DC-DC buck power converter system and effectively reduced the negative impact of sensor noise [6].

An ADRC system consists of three important modules [7]. Tracking differentiator (TD) is chose to smooth the input, the extended state observer (ESO) is designed to observe the disturbance, and nonlinear state error feed-back law (NLSEF) is aimed to get final outputs. Since the ADRC is composed of three parts, which will achieve good results only when appropriate parameters are set, the parameter tuning is of great significance. However, traditional methods depend on rich experience and it is hard to get an optimal result by these approaches. Therefore, it is critical to find an efficient and intelligent method to obtain correct parameters of ADRC system.

Pigeon-inspired optimization (PIO), inspired by the homing behavior of pigeons, was firstly proposed by Duan et al. [8]. Since this novel algorithm has been proved to be effective in improving the convergence speed [9], PIO and its variants have been widely applied to various fields [10–14]. Sun and Pan et al. [10] proposed an effective solution for wireless sensor networks with Quasi-Affine transformation PIO, and Tian and Chu et al. [11] provided an effective solution to the maximum model of short-term power generation of hydropower station with compact PIO. Besides, Wang and Ali et al. [12] utilized a Cauchy mutant PIO to improve the performance of path planning of multiple unmanned aerial vehicles in narrow areas. Moreover, Zhang and Lin et al. [13] applied a novel neural network model based on PIO to predict the parallel branch current of battery pack. In this paper, to enhance the exploration performance for the global optimal solution, the Improved Comprehensive Learning PIO (ICLPIO) is proposed, in which an improved comprehensive learning strategy is applied.

In Sect. 2, the model of HV is described firstly, and then the structure of the ADRC system is introduced. In Sect. 3, as the theoretical basis, the basic PIO algorithm is introduced first and the ICLPIO is proposed. Then, the process of an ICLPIO based parameters tuning method is designed. In Sect. 4, the experiment results with analysis are given. Finally, a brief summary is given in Sect. 5.

2 The ADRC System for HV

2.1 Model of HV

When modeling a HV, longitudinal motion is often the most critical while the lateral movement is relatively with little influence. As a result, the longitudinal model is developed [14], the differential equation of which can be written as Eq. (1). The explanations for parameters are listed in Table 1.

$$\begin{cases} \dot{V} = \frac{T\cos\alpha - D - mg\sin(\theta-\alpha)}{m} \\ \dot{H} = V\sin(\theta-\alpha) \\ \dot{\alpha} = -\frac{L+T\sin\alpha}{mV} + Q + \left(\frac{g}{V} - \frac{V}{r}\right)\cos(\theta-\alpha) \\ \dot{\theta} = Q \\ \dot{Q} = \frac{M}{I_{yy}} \end{cases} \tag{1}$$

Table 1. Explanation of parameters.

Parameter	Explanation	Parameter	Explanation	Parameter	Explanation
m	Mass	I_{yy}	Moment of inertia along the longitudinal direction	L	Lift
V	Velocity	g	Acceleration due to gravity	D	Drag
H	Altitude	δ	Elevator deflection angle	M	Pitching moment
θ	Pitch angle	ϕ	Throttle setting	T	Thrust
Q	Pitch angle rate	α	Attack angle	r	Earth radius

where V, H, θ, Q and α are the state variables. T, L, D and M denote the external forces and moment. The values of vehicle and aerodynamic parameters are consistent with previous studies [14].

2.2 Structure of the ADRC System

The ADRC system is constructed with the structure shown in Fig. 1, including two main part, pitch angle controller and velocity controller. Each controller is consisted of TD, ESO and NLSEF [3]. The reference pitch angle is recorded as θ_{ref}. The reference velocity is V_{ref}. Softened by TD, the reference states are θ_{des}, Q_{des} and V_{des}, which are the desired value of θ, Q and V respectively.

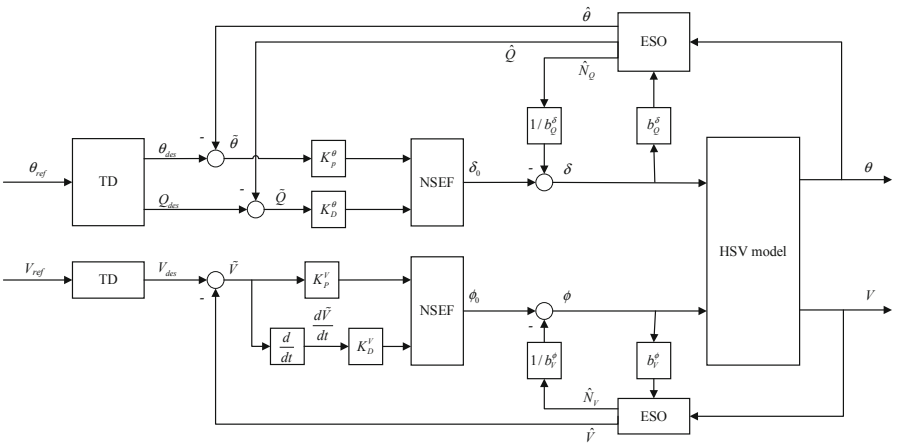

Fig. 1. The structure of the ADRC system.

The softening algorithm can be described as

$$\begin{cases} \dot{\theta}_{des} = Q_{des} \\ \dot{Q}_{des} = -1.76 r_\theta \cdot Q_{des} - r_\theta^2 \left(\theta_{des} - \theta_{ref}\right) \end{cases} \tag{2}$$

$$\ddot{V}_{des} = -1.76 r_V \cdot \dot{V}_{des} - r_V^2 \left(V_{des} - V_{ref}\right) \tag{3}$$

where r_θ and r_V are convergence factors reflecting the softening degree.

The outputs of HSV model θ and V are estimated by ESO. The results are recorded as $\hat{\theta}$, and $\hat{V}$. As the control input δ is the independent variable of pitch angle rate Q, the estimate $\hat{Q}$ is also provided. Besides, all interferences and uncertainties including coupling between inputs and states are estimated as $\hat{N}_Q$, and $\hat{N}_V$. The ESO of pitch angle controller is of second order and the ESO of velocity controller is of first order. The algorithm of ESO is as follow

$$\begin{cases} \tilde{\theta} = \hat{\theta} - \theta \\ \dot{\hat{\theta}} = \hat{Q} - \beta_{11} \cdot \tilde{\theta} \\ \dot{\hat{Q}} = \hat{N}_Q - \beta_{12} \cdot fal\left(\tilde{\theta}, a_{11}, \Delta_{11}\right) + b_1 \delta \\ \dot{\hat{N}}_Q = -\beta_{13} \cdot fal\left(\tilde{\theta}, a_{12}, \Delta_{12}\right) \end{cases} \tag{4}$$

$$\begin{cases} \tilde{V} = \hat{V} - V \\ \dot{\hat{V}} = \hat{N}_V - \beta_{21} \cdot \tilde{V} + b_2 \phi \\ \dot{\hat{N}}_V = -\beta_{22} \cdot fal\left(\tilde{V}, a_2, \Delta_2\right) \end{cases} \tag{5}$$

where β_{11}–β_{22}, a_{11}–a_2 and Δ_{11}–Δ_2 are adjustable parameters with different values. Parameters b_1 and b_2 represent the coefficients of control quantities on corresponding states. By the function $fal(\cdot)$, the input will be enlarged when the absolute value is less than Δ, and otherwise, it will be reduced.

By NLSEF, it is desired that states θ and V reach the softened reference states. The algorithm is shown as

$$\begin{cases} \delta_0 = K_P^\theta \cdot fal\left(\hat{\theta} - \theta, a_\theta, \Delta_\theta\right) + K_D^\theta \cdot fal\left(\hat{Q} - Q, a_Q, \Delta_Q\right) \\ \delta = \delta_0 - \hat{N}_Q \Big/ b_1 \end{cases} \tag{6}$$

$$\begin{cases} \phi_0 = K_P^V \cdot fal\left(\hat{V} - V, a_P^V, \Delta_P^V\right) + K_D^V \cdot fal\left(\hat{Q} - \dot{V}, a_D^V, \Delta_D^V\right) + K_I^V \cdot fal\left(\int \left(\hat{V} - V\right), a_I^V, \Delta_I^V\right) \\ \phi = \phi_0 - \hat{N}_V \Big/ b_2 \end{cases} \tag{7}$$

where K with different corner marks represent the feedback control laws of pitch angle controller and velocity controller respectively.

3 Improved Comprehensive Learning Pigeon-Inspired Optimization

3.1 Basic PIO Algorithm

Inspired by the different stages of characteristics of pigeons when searching the direction of the nest, PIO algorithm is proved to be effective in improving the convergence speed

[8]. Basic PIO consists two independent operators. The first operator is map and compass, and the second is landmark. In the PIO model [9], N solutions is set to the same number of pigeons, and D-dimensional solution space is considered for each pigeon with the position $X_i = [x_{i1}, x_{i2}, \cdots, x_{iD}]$ and the velocity $V_i = [v_{i1}, v_{i2}, \cdots, v_{iD}]$.

In the PIO model, the update process can be described as

$$\begin{cases} V_i(t) = V_i(t-1)e^{-Rt} + rand \cdot \left(X_{gbest} - X_i(t-1)\right) \\ X_i(t) = X_i(t-1) + V_i(t) \end{cases} \tag{8}$$

$$\begin{cases} X_{center}(t) = \dfrac{\sum\limits_{i=1}^{N_N(t)} X_i(t) \cdot fitness(X_i)}{N_N(t) \cdot \sum\limits_{i=1}^{N_N(t)} fitness(X_i)} \\ N_N(t) = \frac{N_N(t-1)}{2} \\ X_i(t) = X_i(t-1) + rand \cdot \left(X_{gbest} - X_i(t-1)\right) \end{cases} \tag{9}$$

For the first operator, pigeons update the position and velocity of the individual with other pigeons especially those with better finesses. For the second operator, the pigeons with worse performance will be eliminated, because when close to the nest, the pigeons who are unfamiliar with the landmarks will not contribute to the team while others will approach the destination in a straight line.

3.2 Improved Comprehensive Learning PIO Algorithm

In the application of basic PIO algorithm, the convergence rate is always competitive, while the deficiency of global search capability is also non-ignorable.

To enhance the exploration performance for the global optimal solution, an improved comprehensive learning strategy is incorporated into basic PIO to improve the search ability [15].

Comprehensive Learning Strategy. In the first operator of the PIO model, each pigeon updates its velocity by the X_{gbest}, which can be far away from the global optimal in a complex application scenario. Besides, one pigeon may get excellent performance in x_{ij} but gets poor fitness because of x_{ik}. Learning from the dimension j of this pigeon could have an active effect on getting the optimal result while it is always neglected in traditional optimization algorithm. To solve these problems, the comprehensive learning strategy for dimension j of pigeon i is described as

$$v_{ij}(t) = v_{ij}(t-1)e^{-Rt} + rand \cdot \left(x_{tar,j} - x_{ij}(t-1)\right) \tag{10}$$

where x_{tar} is a randomly selected pigeon, which improves the utilization of all pigeon information.

Selective Learning Mechanism. Equation (10) proposed the learning method from a randomly selected pigeon, rather than the pigeon with best fitness. This strategy obviously improves the global information but will limit the convergence speed greatly. Therefore, based on the comprehensive learning strategy, a selective learning mechanism is proposed. The mechanism is mainly divided into three aspects [16].

1) To avoid the disordered learning, a learning interval T_{in} is considered, which means that there is a refreshing gap for pigeons to choose their learning target.
2) For each pigeon, a probability P_c^i is set by $P_c^i = 0.05 + 0.45 \cdot \frac{\exp\left(\frac{10(i-1)}{P_s-1}-1\right)}{\exp(10)-1}$, where P_s is the whole number of pigeons. A random number $p_c^{i,j}$ is considered before the velocity update. Only if the $p_c^{i,j}$ is greater than the P_c^i, the comprehensive learning strategy will be used.
3) Due to the randomness of the learning target, the better result cannot be guaranteed. Therefore, two pigeons will be selected randomly and then the one with better fitness is to choose as the target individual.

3.3 Optimized ADRC System for HV

As shown in Fig. 2, the whole process of the ICLPIO optimized ADRC system for HV can be described as follows.

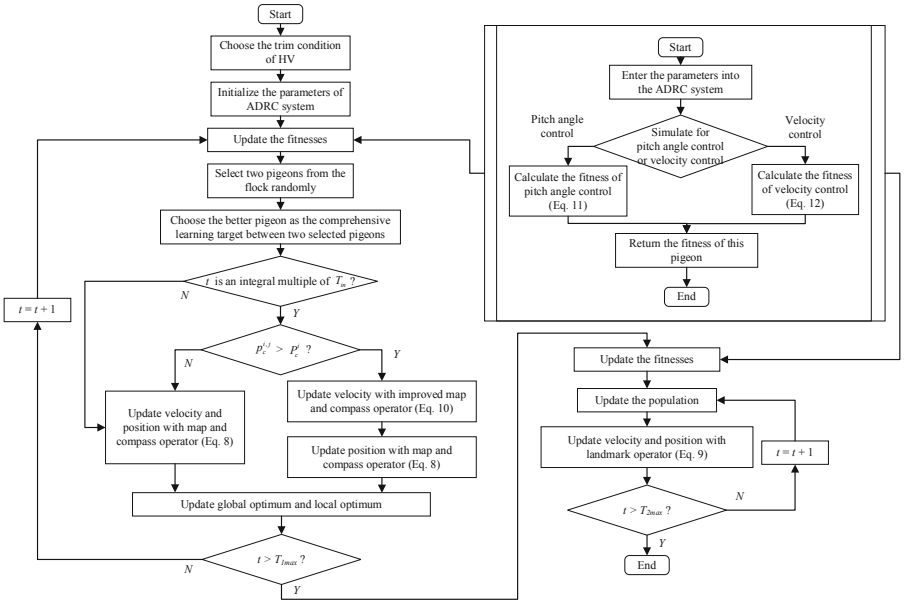

Fig. 2. Flowchart of the ICLPIO.

Step 1: Choose the trim condition of HV, including choosing the stable state variables and the appropriate external forces and moment.
Step 2: Initialize the parameters of ADRC system.
Step 3: Implement the simulation and calculate the fitness for pitch angle control by Eq. (11) and that for velocity control by Eq. (12).
Step 4: Select two pigeons randomly and choose the better one as the comprehensive learning target.

Step 5: Update the velocity and position of each pigeon. If current iteration times t is an integral multiple of the learning interval T_{in}, and the $p_c^{i,j}$ is greater than the P_c^i, the learning target for pigeon i is the one chosen by Step 4. Otherwise, the global optimum will be chosen as the target.
Step 6: If t reaches the $T_{1\max}$, update the velocity and position with landmark operator by Eq. (9). Otherwise, go to Step 3.
Step 7: If t reaches the $T_{2\max}$, terminal the optimization and output the result.

$$fitness_p = \int t \cdot \frac{|\theta_{ref} - \theta|}{\theta_{ref}} dt \tag{11}$$

$$fitness_v = \int t \cdot \frac{|V_{ref} - V|}{V_{ref}} dt \tag{12}$$

4 Simulation Results and Analysis

For tuning the parameters of controller, the number of iterations is set to 35 times, where it is selected 30 times for the first operator and 5 times for the second operator both in PIO and ICLPIO. The number of solutions is 20, and the dimension of each solution is 14. For pitch angle controller, $\{r_\theta, \beta_{11}, \beta_{12}, \beta_{13}, a_\theta, \Delta_\theta, a_Q, \Delta_Q, K_P^\theta, K_D^\theta, a_{11}, \Delta_{11}, a_{12}, \Delta_{12}\}$ are optimized, and for velocity controller, $\{r_V, \beta_{21}, \beta_{22}, a_P^V, \Delta_P^V, a_I^V, \Delta_I^V, a_D^V, \Delta_D^V, K_P^V, K_I^V, K_D^V, a_2, \Delta_2\}$ are optimized.

To verify the ability to find the global optimum of the proposed algorithm ICLPIO, comparative simulations are carried out. As control groups, the particle swarm optimization (PSO), the basic PIO, and the genetic algorithm (GA) are applied in the simulations. During the experiments, the reference of pitch angle is chosen as 5 degrees, and the reference of velocity is chosen as 200 m per second. The individual optimal iteration diagrams are shown in Fig. 3.

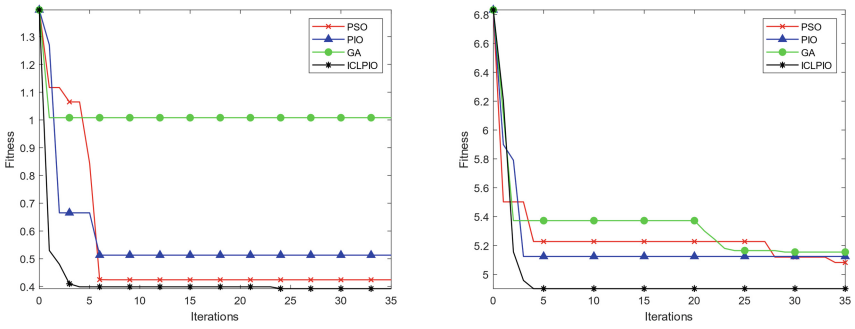

Fig. 3. Optimal individual fitness of pitch angle controller (left) and velocity controller (right).

By the results, the fitness found by the ICLPIO is always the lowest, which shows the best global search capability.

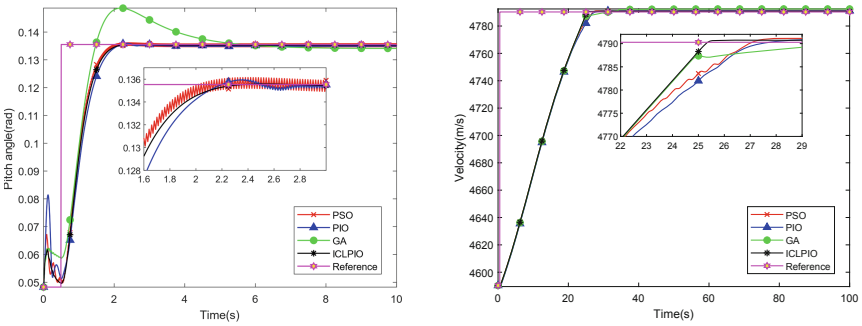

Fig. 4. Response of pitch angle control (left) and velocity control (right).

As the optimal solution, the response curves to the reference inputs of the ADRC system with parameters optimized by ICLPIO and other three algorithms are shown in Fig. 4.

For pitch angle control, the adjustment time of ICLPIO is 1.19 s, which of the PSO, PIO, and GA are 1.12 s, 1.26 s, and 3.29 s, respectively. The overshoots of ICLPIO and PSO are both zero, while that of PIO and GA are 0.46 percent and 15 percent. Only the result optimized by ICLPIO has no oscillation.

For velocity control, the adjustment time in pitch angle control of ICLPIO is 24.26 s. The results of PSO, PIO, and GA are 25.64 s, 25.68 s, and 24.30 s, respectively. The result of ICLPIO has the smallest steady-state error.

5 Conclusion

In this paper, an ADRC system is designed to address the disturbance for HV. To track the reference input accurately, with the comprehensive learning strategy and the selective learning mechanism, the ICLPIO algorithm is proposed. To verify the ability to find the global optimum, comparative simulations are carried out and the results show that, the ICLPIO achieves competitive dynamic and steady-state performances in the pitch angle control and velocity control of HV.

Acknowledgements. This work was partially supported by Science and Technology Innovation 2030-Key Project of "New Generation Artificial Intelligence" under grant #2018AAA0102403, National Natural Science Foundation of China under grant #91948204, #U20B2071.

References

1. Ding, Y., Wang, X., Bai, Y.: An improved continuous sliding mode controller for flexible air-breathing hypersonic vehicle. Int. J. Robust Nonlinear Control **30**(5), 5751–5772 (2020)
2. Wang, L., Qi, R., Jiang, B.: Adaptive actuator fault-tolerant control for non-minimum phase air-breathing hypersonic vehicle model. ISA Trans. https://doi.org/10.1016/j.isatra.2021.07.032

3. Fareh, R., Khadraoui, S., Abdallah, M., et al.: Active disturbance rejection control for robotic systems: a review. Mechatronics. https://doi.org/10.1016/j.mechatronics.2021.102671
4. Gao, T., Tang, R., Rao, J., et al.: On-line adaptive controller system used on small UAV. Procedia Eng. **45**, 980–985 (2012)
5. Luo, S., Sun, Q., Wu, W., et al.: Accurate flight path tracking control for powered parafoil aerial vehicle using ADRC-based wind feedforward compensation. Aerosp. Sci. Technol. **84**, 904–915 (2019)
6. Krzysztof, L., Rafal, M., Bin, D., et al.: Active disturbance rejection control design with suppression of sensor noise effects in application to DC-DC buck power converter. IEEE Trans. Ind. Electron. **69**(1), 816–824 (2022)
7. Li, Y., Chen, Z., Sun, M., Liu, Z., Zhang, Q.: ADRC based attitude control of a quad-rotor robot. In: Deng, Z., Li, H. (eds.) Lecture Notes in Electrical Engineering, vol. 337, pp. 503–512. Springer, Heidelberg (2015). https://doi.org/10.1007/978-3-662-46463-2_5
8. Duan, H., Qiao, P.: Pigeon-inspired optimization: a new swarm intelligence optimizer for air robot path planning. Int. J. Intell. Comput. Cybern. **7**(1), 24–37 (2014)
9. Duan, H., Qiu, H.: Advancements in pigeon-inspired optimization and its variants. Sci. China Inf. Sci. **62**(7), 070201:1–070201:10 (2019)
10. Sun, X., Pan, J., Chu, S., et al.: A novel pigeon-inspired optimization with quasi-Affine transformation evolutionary algorithm for DV-Hop in wireless sensor networks. Int. J. Distrib. Sens. Netw. **16**(6), 62–77 (2020)
11. Tian, A., Chu, S., Pan, J., et al.: A compact pigeon-inspired optimization for maximum short-term generation mode in cascade hydroelectric power station. Sustainability **12**(3), 40–58 (2020)
12. Wang, B., Wang, D., Ali, Z.: A Cauchy mutant pigeon-inspired optimization–based multi-unmanned aerial vehicle path planning method. Meas. Control **53**(1), 83–92 (2020)
13. Zhang, Y., Lin, S., Ma, H., et al.: A novel pigeon-inspired optimized RBF model for parallel battery branch forecasting. Complexity. https://doi.org/10.1155/2021/8895496
14. Li, P., Huang, P., He, C., et al.: Finite-time dynamic surface fault-tolerant control for hypersonic vehicle with mismatched disturbances. Int. J. Control Autom. Syst. **19**(7), 2309–2322 (2021)
15. Sun, Y., Duan, H., Xian, N.: Fractional-order controllers optimized via heterogeneous comprehensive learning pigeon-inspired optimization for autonomous aerial refueling hose–drogue system. Aerosp. Sci. Technol. **81**, 1–13 (2018)
16. Liang, J., Qin, A., Suganthan, P., et al.: Comprehensive learning particle swarm optimizer for global optimization of multimodal functions. IEEE Trans. Evol. Comput. **10**(3), 281–295 (2006)